The current issue and full text archive of this journal is available at
www.emeraldinsight.com/0961-5539.htm



# Analysis of conduction-radiation problem in absorbing and emitting nongray materials

Severino P.C. Marques
*Center of Technology, Federal University of Alagoas, Maceió, Alagoas, Brazil, and*
Ever J. Barbero and John S.R. Murillo
*Department of Mechanical and Aerospace Engineering, West Virginia University, Morgantown, West Virginia, USA*

Received 14 April 2007
Revised 21 November 2007
Accepted 19 December 2007

## Abstract

**Purpose** – The purpose of this paper is to present a computationally efficient model to solve combined conduction/radiation heat transfer problems in absorbing, emitting, non-scattering, non-gray materials.

**Design/methodology/approach** – The model is formulated for steady-state condition and based on an iterative approach where the medium is discretized into finite strips and the extinction spectrum is divided into finite bands to consider the extinction coefficient variation with the wavelength.

**Findings** – Temperature fields and heat flux distributions are presented to demonstrate the capability of the formulation. It is shown that the model is quite accurate and efficient even for the cases of pure radiation. Differently from other models, the number of iterations required by the model for convergence is very low, even in the cases dominated by radiation.

**Originality/value** – The model has great potential to contribute with the evaluation and design of materials for thermal insulation, where radiation heat transfer can be the dominant mechanism, such as aerogel materials which are recognized as the solids with the lowest thermal conductivity and are intended to be used in building and construction, aerospace, transportation and other applications.

**Keywords** Numerical analysis, Thermal properties of materials, Heat transfer
**Paper type** Research paper

## Nomenclature

| | |
|---|---|
| C | constant value |
| $d$ | thickness of a strip |
| $D$ | thickness of the sample |
| $E$ | exponential integral function |
| $i$ | spectral radiation intensity |
| $K$ | extinction coefficient |
| $L$ | total number of strips |
| $M$ | total number of spectrum bands |
| N | conduction–radiation parameter |
| $q$ | heat flux |
| T | temperature, coefficient of temperature fields |
| $x$ | global Cartesian coordinate |
| $\bar{x}$ | local Cartesian coordinate |
| $\alpha$ | generic number of a strip |
| $\beta$ | thermal conductivity |
| $\varepsilon$ | boundary emissivity |
| $\zeta$ | non-dimensional flux |
| $\eta$ | refractive index |
| $\Theta$ | non-dimensional temperature |

The first author would like to gratefully acknowledge the financial support of the Brazilian federal agency CNPq.

International Journal of Numerical Methods for Heat & Fluid Flow
Vol. 19 No. 2, 2009
pp. 165-181

0961-5539
DOI 10.1108/09615530910930955

$\kappa$ optical coordinate
$\lambda$ wavelenght
$\mu$ cosine of radiation direction
$\sigma$ Stefan–Boltzmann constant
$\psi$ equation of the non-linear system

*Subscript*

$b$ blackbody
$c$ conduction
$i,j,\gamma$ indices
$m$ iterative step
$n$ order of the exponential integral function
$r$ radiation
$t$ total

*Superscript*

$+$ in forward direction
$-$ in backward direction
$*$ optical coodinate for integration
$'$ directional spectral radiation intensity

## Introduction

Combined conduction and radiation heat transfer mechanisms are encountered in many important practical applications, such as design of furnaces, manufacturing of glass, fiber and foam insulations, studies of filler and cover for special windows and solar collectors, and so on. Many interesting materials for these applications present complex radiative behaviors which can be strongly dependent on the electromagnetic spectrum, such as aerogels and other special foams. These materials are classified as non-gray materials.

Several numerical and experimental studies exist for the analysis of heat transfer by simultaneous conduction and radiation in gray materials; that is, materials with extinction coefficient independent of wavelength. Theoretical models for heat transfer involving radiation have been recognized as computationally expensive (Daurelle *et al.*, 1999; Marakis *et al.*, 2001; Mishra *et al.*, 2006). The difficulty and high processing cost of radiation problems are due to the integro-differential nature of its governing equations (Siegel and Howell, 2002). However, efforts have been directed to reduce the processing time by developing new models and improving the computational efficiency of the existing ones (Ratzell III and Howell, 1982; Manzari, 1998; Coelho and Gonçalves,1999; Anteby *et al.*, 2000; Mishra *et al.*, 2004). A pioneer theoretical formulation for this problem was presented by Viskanta and Grosh (1962a). These authors obtained a rigorous solution for the case of one-dimensional gray medium using a complex transformation of the integro-differential equation into a non-linear integral equation which is solved by an iterative procedure. They also used their formulation to investigate the effect of boundary emissivities on heat transfer in gray medium (Viskanta and Grosh, 1962b). More recently, the discrete transfer method (Shah, 1979) and the collapsed dimension method (Mishra and Prasad, 2002) address the same problem. Comparisons of results obtained by these last methods are presented in Talukdar and Mishra (2002). The results are in very good agreement with those published by Viskanta and Grosh (1962a, b), but the number of iterations required for radiation dominated problems are very large. According to the authors, an under relaxation technique is required for convergence when the conduction–radiation parameter is smaller or equal to 0.01.

A review in the literature shows that most of the published models are concerned with heat transfer in gray medium. For the case of non-gray medium, it can be cited the theoretical–experimental work by (Heinemann *et al.*, 1996), in which a numerical model

is used to describe combined conduction and radiation heat transfer in silica aerogels. However, the information about the theoretical model presented in (Heinemann *et al.*, 1996) is insufficient to reproduce its results.

In the present work a model for the analysis of heat transfer by simultaneous conduction and radiation mechanisms in one-dimensional planar non-gray medium is presented. The main features of this model are its simplicity and fastness for convergence. It is based on a finite strip theory and its basic idea already has been used to solve linear mechanical and thermal conduction problem for heterogeneous materials (Cavalcante *et al.*, 2007). Here, the model consists of an iterative tangent non-linear formulation in which the medium is discretized into finite strips and the extinction spectrum is divided into finite bands. Inside each strip the temperature field is approximated using quadratic expansions in local coordinates whose coefficients are the primary unknowns of the problem. The discrete expressions of the model consist of balance energy equations and continuity conditions of temperature and heat flux. For verification, the model is applied to solve problems including gray and non-gray participating media with different thermal and optical properties and temperature conditions. In the examples, silica aerogels are selected as non-gray materials. Results of temperature fields and conductive, radiative and total heat fluxes are presented and the relative importance of the heat transfer modes can clearly be seen. Comparison of results with others obtained by different theoretical models demonstrates the very good performance of the formulation from accuracy and number of iterations for convergence.

## Theoretical formulation

The basic equations of the problem to be solved are described in this section. A planar sample of a homogeneous, isotropic, non-gray material limited by two boundary surfaces is shown in Figure 1. The material is absorbing, emitting, and non-scattering, whereas the boundaries 1 and 2 are opaque and diffuse surfaces. The temperature values on the boundaries 1 and 2 are denoted by $T_1$ and $T_2$, respectively. Heat transfer inside the material occurs by conduction and radiation. The material properties are independent of temperature.

Under steady-state condition, the total heat flux $q_t$ is constant through the thickness $D$ of the sample and given by

$$q_t = q_c(x) + q_r(x) \tag{1}$$

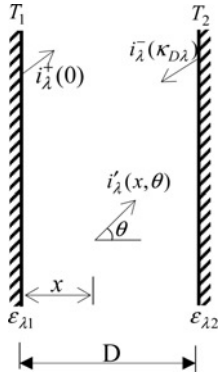


**Figure 1.**
Absorbing-emitting material between two diffuse boundary surfaces

where $q_c(x)$ and $q_r(x)$ indicate the values of the conductive and radiative fluxes, respectively, occurring on the point with coordinate $x$ (Figure 1). The conductive flux is obtained by Fourier's law

$$q_c(x) = -\beta_c \frac{dT}{dx} \tag{2}$$

where $T$ represents temperature and $\beta_c$ is the thermal conductivity of the material. The radiative flux is defined by (Siegel and Howell, 2002) as

$$q_r(x) = \int_0^\infty dq_{r\lambda}(x) = \int_0^\infty \frac{\partial q_{r\lambda}(x)}{\partial \lambda} d\lambda \tag{3}$$

with $q_{r\lambda}$ being the radiative flux corresponding to wavelength $\lambda$.

Introducing the optical coordinate $\kappa_\lambda = K_\lambda x$, where $K_\lambda$ is the material's extinction coefficient (which, for non-gray materials is a function of the radiation wavelength $\lambda$), the derivative in Equation (3) can be written as (Siegel and Howell, 2002)

$$\begin{aligned}\frac{\partial q_{r\lambda}}{\partial \lambda} = {} & 2\pi i_\lambda^+(0) \int_0^1 \exp\left(-\frac{\kappa_\lambda}{\mu}\right)\mu\, d\mu - 2\pi i_\lambda^-(\kappa_{D\lambda}) \\ & \times \int_0^1 \exp\left(-\frac{\kappa_{D\lambda} - \kappa_\lambda}{\mu}\right)\mu\, d\mu \\ & + 2\pi \int_0^{\kappa_\lambda} \eta_\lambda^2 i'_{b\lambda}(\kappa_\lambda^*) E_2(\kappa_\lambda - \kappa_\lambda^*) d\kappa_\lambda^* \\ & - 2\pi \int_{\kappa_\lambda}^{\kappa_{D\lambda}} \eta_\lambda^2 i'_{b\lambda}(\kappa_\lambda^*) E_2(\kappa_\lambda^* - \kappa_\lambda) d\kappa_\lambda^*\end{aligned} \tag{4}$$

In this equation, $i_\lambda^+(0)$ and $i_\lambda^-(\kappa_{D\lambda})$ represent the forward and backward intensities (both functions of wavelengths) at boundaries 1 and 2, respectively, $\kappa_{D\lambda}$ is the optical thickness of the sample and $\eta_\lambda$ is the material's refractive index. Furthermore, $\mu = \cos\theta$, with $\theta$ the angle between the radiation direction and the $x$-axis (Figure 1). The blackbody radiation intensity $i'_{b\lambda}$ (also a function of $\lambda$) depends on the temperature and it is computed by Planck's law

$$i'_{b\lambda} = \frac{2C_1}{\lambda^5 (e^{C_2/\lambda T} - 1)} \tag{5}$$

where $C_1$ and $C_2$ are constants. The symbol $E_2()$ in Equation (4) is a particular case of the integral

$$E_n(\xi) = \int_0^1 \mu^{n-2} e^{-\xi/\mu}\, d\mu \tag{6}$$

for $n = 2$. The intensities at the boundaries can be evaluated by the following expressions

$$i_\lambda^+(0) = \varepsilon_{\lambda 1} n_\lambda^2 i'_{b\lambda,1} + 2(1-\varepsilon_{\lambda 1})\left[i_\lambda^-(\kappa_{D\lambda}) E_3(\kappa_{D\lambda}) + \int_o^{\kappa_{D\lambda}} n_\lambda^2 i'_{b\lambda}(\kappa_\lambda^*) E_2(\kappa_\lambda^*) d\kappa_\lambda^*\right] \tag{7}$$

and

$$i_\lambda^-(\kappa_{D\lambda}) = \varepsilon_{\lambda 2} n_\lambda^2 i'_{b\lambda,2} + 2(1-\varepsilon_{\lambda 2})\left[i_\lambda^+(0) E_3(\kappa_{D\lambda}) + \int_o^{\kappa_{D\lambda}} n_\lambda^2 i'_{b\lambda}(\kappa_\lambda^*) E_2(\kappa_{D\lambda} - \kappa_\lambda^*)\, d\kappa_\lambda^*\right] \tag{8}$$

where $\varepsilon_{\lambda 1}$ and $\varepsilon_{\lambda 2}$ are the emissivities of the boundary surfaces 1 and 2, respectively, which are functions of wavelength $\lambda$.

For conduction–radiation heat transfer, the energy conservation equation governing the problem is given by

$$\nabla \cdot (\beta_c \nabla T - q_r) = 0 \tag{9}$$

which can be written in the form of an integro-differential equation as

$$\beta_c \frac{d^2 T}{dx^2} - \int_0^\infty K_\lambda \frac{\partial^2 q_{r\lambda}}{\partial \kappa_\lambda \partial \lambda}\, d\lambda = 0 \tag{10}$$

Using Equation (4), the following expression can be derived (Siegel and Howell, 2002)

$$\frac{\partial^2 q_{r\lambda}}{\partial \kappa_\lambda d\lambda} = -2\pi i_\lambda^+(0) \int_0^1 \exp\left(-\frac{\kappa_\lambda}{\mu}\right) d\mu - 2\pi i_\lambda^-(\kappa_{D\lambda}) \int_0^1 \exp\left(-\frac{\kappa_{D\lambda} - \kappa_\lambda}{\mu}\right) d\mu - 2\pi \int_0^{\kappa_\lambda} \eta_\lambda^2 i'_{b\lambda}(\kappa_\lambda^*) E_1(\kappa_\lambda - \kappa_\lambda^*)\, d\kappa_\lambda^* - 2\pi \int_{\kappa_\lambda}^{\kappa_{D\lambda}} \eta_\lambda^2 i'_{b\lambda}(\kappa_\lambda^*) E_1(\kappa_\lambda^* - \kappa_\lambda)\, d\kappa_\lambda^* + 4\pi \eta_\lambda^2 i'_{b\lambda}(\kappa_\lambda) \tag{11}$$

## Numerical formulation

The problem to be solved is governed by the integro-differential Equation (10) with the boundary conditions $T(0) = T_1$ and $T(D) = T_2$. This is a non-linear and non-local problem whose solution presents difficulties because the divergence of the radiative heat flux in Equation (11) depends on the temperature field which is not known a priory. The problem is non-local because the heat flux depends not only on the temperature gradient at the point but also on the all temperature field.

In the present formulation, the integral of Equation (10) is approximated by a summation. The total wavelength interval is divided into $M$ small subintervals $[\lambda_j, \lambda_{j+1}]$ with flexible widths $\Delta\lambda_j = \lambda_{j+1} - \lambda_j$, where $1 \le j \le M$. Each subinterval $j$ is associated with single values of extinction coefficient $K_{\lambda j}$ and refractive index $n_{\lambda j}$, as

shown in Figure 2. Hence, the energy Equation (9) is written as

$$\beta_c \frac{d^2T}{dx^2} - \sum_{j=1}^{M} K_{\lambda j} \left( \frac{\partial^2 q_{r\lambda}}{\partial \kappa_\lambda d\lambda} \right)_j \Delta\lambda_j = 0 \tag{12}$$

To obtain discrete equations, the sample is divided into $L$ strips with variable thickness $d_\alpha$ $(1 \le \alpha \le L)$ as shown in Figure 3. A local coordinate $\bar{x}^{(\alpha)}$ is attached to the strip's center, so that $-\frac{d_\alpha}{2} \le \bar{x}^{(\alpha)} \le \frac{d_\alpha}{2}$.

The temperature field is approximated in each strip using a quadratic expansion in the corresponding local coordinate. Then, for the $\alpha-$strip, the temperature field is given by

$$T(\bar{x}) = T_o^{(\alpha)} + \bar{x} T_1^{(\alpha)} + \frac{1}{2}\left(3\bar{x}^2 - \frac{d_\alpha^2}{4}\right) T_2^{(\alpha)} \tag{13}$$

where $T_o^{(\alpha)}$, $T_1^{(\alpha)}$ and $T_2^{(\alpha)}$ are the unknown temperature coefficients of the $\alpha-$strip. In Equation (13), $T_o^{(\alpha)}$ represents the mean temperature on the $\alpha-$strip and $\beta_c T_1^{(\alpha)}$ is the conduction flux at the center of the $\alpha-$strip. Using this approximated temperature field, the divergence of the conductive flux can be written as

$$\frac{dq_c}{dx} = \frac{dq_c}{d\bar{x}} = -3\beta_c T_2^{(\alpha)} \tag{14}$$

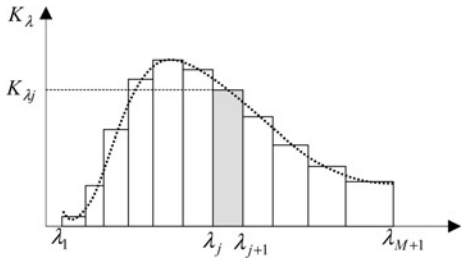


**Figure 2.**
Extinction spectrum divided into $M$ wavelength subintervals

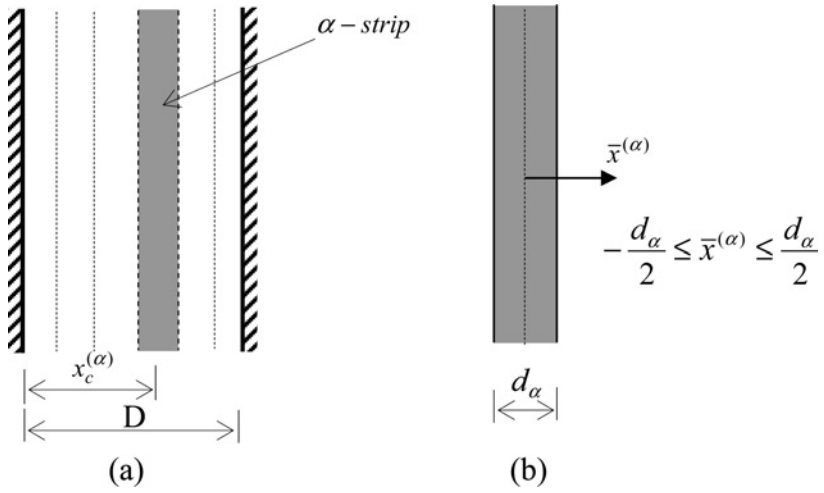


**Figure 3.**
(a) Material sample divided into $L$ strips and (b) local coordinate system for the $\alpha-$strip

Hence, using Equations (11) and (14), the energy Equation (9) written for the center ($\bar{x}^{(\alpha)} = 0$) of the $\alpha-$strip can be given by the following expression

$$\psi_\alpha = 3\beta_c T_2^{(\alpha)} + 2\pi \sum_{j=1}^{M} K_{\lambda j} \times [i_\lambda^+(0) E_2(\kappa_{c\lambda}^{(\alpha)}) + i_\lambda^-(\kappa_{D\lambda}) E_2(\kappa_{D\lambda} - \kappa_{c\lambda}^{(\alpha)}) + \eta_{\lambda j}^2 \sum_{\gamma=1}^{\alpha-1} \int_{\kappa_{1\lambda}^{(\gamma)}}^{\kappa_{2\lambda}^{(\gamma)}} i'_{b\lambda}(\kappa_\lambda^*) E_1(\kappa_{c\lambda}^{(\alpha)} - \kappa_\lambda^*)\, d\kappa_\lambda^* + \eta_{\lambda j}^2 \int_{\kappa_{1\lambda}^{(\alpha)}}^{\kappa_{2\lambda}^{(\alpha)}} i'_{b\lambda}(\kappa_\lambda^*) E_1(|\kappa_{c\lambda}^{(\alpha)} - \kappa_\lambda^*|)\, d\kappa_\lambda^* + \eta_{\lambda j}^2 \sum_{\gamma=\alpha+1}^{L} \int_{\kappa_{1\lambda}^{(\gamma)}}^{\kappa_{2\lambda}^{(\gamma)}} i'_{b\lambda}(\kappa_\lambda^*) E_1(\kappa_\lambda^* - \kappa_{c\lambda}^{(\alpha)})\, d\kappa_\lambda^* - 2\eta_{\lambda j}^2 i'_{b\lambda}(\kappa_{c\lambda}^{(\alpha)})] \Delta\lambda_j = 0 \tag{15}$$

where $\kappa_{c\lambda}^{(\alpha)}$ is the optical coordinate of the center of the strip. The derivatives of $\psi_\alpha$ with respect to the unknown temperature coefficients $T_o^{(\gamma)}$, $T_1^{(\gamma)}$ and $T_2^{(\gamma)}$, associated with the $\gamma-$strip, are given by

$$\frac{\partial \psi_\alpha}{\partial T_o^{(\gamma)}} = 2\pi \sum_{j=1}^{M} K_{\lambda j} \left[ \frac{\partial i_\lambda^+(0)}{\partial T_o^{(\gamma)}} E_2(\kappa_{c\lambda}^{(\alpha)}) + \frac{\partial i_\lambda^-(\kappa_{D\lambda})}{\partial T_o^{(\gamma)}} E_2\left(\kappa_{D\lambda} - \kappa_{c\lambda}^{(\alpha)}\right) + \eta_{\lambda j}^2 \int_{\kappa_{1\lambda}^{(\gamma)}}^{\kappa_{2\lambda}^{(\gamma)}} \frac{\partial i'_{b\lambda}(\kappa_\lambda^*)}{\partial T} E_1\left(\left|\kappa_{c\lambda}^{(\alpha)} - \kappa_\lambda^*\right|\right) d\kappa_\lambda^* - 2\eta_{\lambda j}^2 \delta_{\alpha\gamma} \frac{\partial i'_{b\lambda}(\kappa_{c\lambda}^{(\alpha)})}{\partial T} \right] \Delta\lambda_j = 0 \tag{16}$$

and

$$\frac{\partial \psi_\alpha}{\partial T_1^{(\gamma)}} = 2\pi \sum_{j=1}^{M} K_{\lambda j} \left[ \frac{\partial i_\lambda^+(0)}{\partial T_1^{(\gamma)}} E_2(\kappa_{c\lambda}^{(\alpha)}) + \frac{\partial i_\lambda^-(\kappa_{D\lambda})}{\partial T_1^{(\gamma)}} E_2\left(\kappa_{D\lambda} - \kappa_{c\lambda}^{(\alpha)}\right) + \eta_{\lambda j}^2 \int_{\kappa_{1\lambda}^{(\gamma)}}^{\kappa_{2\lambda}^{(\gamma)}} \frac{\partial i'_{b\lambda}(\kappa_\lambda^*)}{\partial T} \bar{x}^{(\gamma)} E_1\left(\left|\kappa_{c\lambda}^{(\alpha)} - \kappa_\lambda^*\right|\right) d\kappa_\lambda^* - 2\eta_{\lambda j}^2 \delta_{\alpha\gamma} \frac{\partial i'_{b\lambda}(\kappa_{c\lambda}^{(\alpha)})}{\partial T} \bar{x}^{(\gamma)} \right] \Delta\lambda_j = 0 \tag{17}$$

and

$$\frac{\partial \psi_\alpha}{\partial T_2^{(\gamma)}} = 3\beta_c \delta_{\alpha\gamma} + 2\pi \sum_{j=1}^{M} K_{\lambda j} \left[ \frac{\partial i_\lambda^+(0)}{\partial T_2^{(\gamma)}} E_2(\kappa_{c\lambda}^{(\alpha)}) + \frac{\partial i_\lambda^-(\kappa_{D\lambda})}{\partial T_2^{(\gamma)}} E_2(\kappa_{D\lambda} - \kappa_{c\lambda}^{(\alpha)}) + \eta_{\lambda j}^2 \int_{\kappa_{1\lambda}^{(\gamma)}}^{\kappa_{2\lambda}^{(\gamma)}} \frac{\partial i'_{b\lambda}(\kappa_\lambda^*)}{\partial T} \frac{1}{2} \left( 3\bar{x}^{(\gamma)2} - \frac{d_\gamma^2}{4} \right) E_1\left(\left|\kappa_{c\lambda}^{(\alpha)} - \kappa_\lambda^*\right|\right) d\kappa_\lambda^* - \eta_{\lambda j}^2 \delta_{\alpha\gamma} \frac{\partial i'_{b\lambda}(\kappa_{c\lambda}^{(\alpha)})}{\partial T} \left( 3\bar{x}^{(\gamma)2} - \frac{d_\gamma^2}{4} \right) \right] \Delta\lambda_j = 0 \tag{18}$$

where $\delta_{\alpha\gamma}$ stands for the Kronecker delta.

Assuming narrow strips, the blackbody radiation intensities and their derivatives appearing in Equations (16)-(18), can be approximately evaluated in terms of the mean temperature values $T_o$ on the strips. Using this simplification, the integrals over the optical coordinate can be solved explicitly. Here, the integrals of the type $E_n$ are obtained by four-point Gaussian quadrature. The numerical model results in $L$ energy equations, one for each strip. These equations depend on the unknown temperature coefficients.

Additional equations are given by the compatibility conditions of flux and temperature on the ends of the strips, as follows:

Temperature compatibility at the interfaces between adjacent strips

$$T^{(\alpha-1)}\left(\bar{x}=\frac{d_{\alpha-1}}{2}\right)=T^{(\alpha)}\left(\bar{x}=-\frac{d_{\alpha}}{2}\right)$$

$$T_o^{(\alpha-1)}+\frac{d_{\alpha-1}}{2}T_1^{(\alpha-1)}+\frac{d_{\alpha-1}^2}{4}T_2^{(\alpha-1)}=T_o^{(\alpha)}-\frac{d_{\alpha}}{2}T_1^{(\alpha)}+\frac{d_{\alpha}^2}{4}T_2^{(\alpha)} \tag{19}$$

Conduction heat flux compatibility at the interfaces between adjacent strips

$$q_c^{(\alpha-1)}\left(\bar{x}=\frac{d_{\alpha-1}}{2}\right)=q_c^{(\alpha)}\left(\bar{x}=-\frac{d_{\alpha}}{2}\right)$$

$$T_1^{(\alpha-1)}+\frac{3d_{\alpha-1}}{2}T_2^{(\alpha-1)}=T_1^{(\alpha)\prime}-\frac{3d_{\alpha}}{2}T_2^{(\alpha)} \tag{20}$$

Temperature boundary conditions

$$T_o^{(1)}-\frac{d_1}{2}T_1^{(1)}+\frac{d_1^2}{4}T_2^{(1)}=T_1$$

$$T_o^{(L)}+\frac{d_L}{2}T_1^{(L)}+\frac{d_L^2}{4}T_2^{(L)}=T_2 \tag{21}$$

A non-linear system with $3L$ equations and $3L$ unknown temperature coefficients is given by Equations (15), (19)-(21). An iterative solution is used to solve this problem. In general, the equations of the non-linear system can be written as

$$\psi_i\left(\vec{T}\right)=0(i=1,2,\ldots,3L) \tag{22}$$

where $\vec{T}$ is the vector of temperature coefficients given by

$$\vec{T}=\left\{T_o^{(1)}T_1^{(1)}T_2^{(1)}T_o^{(2)}T_1^{(2)}T_2^{(2)},\ldots,T_o^{(L)}T_1^{(L)}T_2^{(L)}\right\} \tag{23}$$

Considering Taylor's series expansion of $\psi_i$ on the vector $\vec{T}_m$, corresponding to certain iteration $m$ and neglecting higher order terms, a linearization of the problem is

represented as follows

$$\psi_i\left(\vec{T}_{m+1}\right) \approx \psi_i\left(\vec{T}_m\right) + \left(\frac{\partial \psi_i}{\partial \vec{T}}\right)_{\vec{T}=\vec{T}_m} \cdot \delta\vec{T}_m = 0 \tag{24}$$

where $\left(\frac{\partial \psi_i}{\partial \vec{T}}\right)$ represents the Jacobian matrix of the function $\psi_i$ and $\delta\vec{T}_m$ indicates the increment vector of temperature coefficients defined by

$$\delta\vec{T}_m = \vec{T}_{m+1} - \vec{T}_m \tag{25}$$

Using Equations (24) and (25), the unknown temperature coefficients are obtained iteratively, as follows

$$\vec{T}_{m+1} = \vec{T}_m - \left(\frac{\partial \psi_i}{\partial \vec{T}}\right)^{-1}_{\vec{T}=\vec{T}_m} \cdot \psi_i\left(\vec{T}_m\right) = 0 \tag{26}$$

The iterative process starts with an initial temperature field, calculated as the conduction-only heat transfer problem. Convergence is achieved when the Euclidean norm of the $n$th increment of the temperature field normalized by the temperature field is less than a tolerance, usually set to $10^{-3}$. Convergence is extremely fast, even for non-gray materials, when compared with previous algorithms, which were applied to gray materials only. Gray materials present less difficulty because the wavelength dependency is eliminated.

**Verification for gray materials**

The accuracy of the algorithm is demonstrated by comparing with results available in the literature for gray materials. The conduction–radiation parameter is defined by $N = \beta_c K/4\sigma T_{ref}^3$, where $K$ is the extinction coefficient, $T_{ref}$ is a reference temperature and $\sigma$ is the Stefan–Boltzmann constant ($\sigma = 5.6696 \times 10^{-8}\mathrm{W/m^2K^4}$). Here, $T_{ref}$ has been taken as the maximum temperature on the boundary ($T_1 or T_2$). For high values of $N$, conduction is the dominating heat transfer mechanism, whereas for small values of $N$, radiation dominates.

Figures 4(a) and (b) present non-dimensional temperature distributions ($\Theta = T/T_1$) for optical thickness $\kappa_D = 1$, $T_2/T_1 = 0.5$ and different values of $N$ and boundary emissivities. In Figure 4(a), results for $N = 0.0, 0.01, 0.1, 10$ and boundary emissivity $\varepsilon = 1.0$ are compared with those obtained by (Talukdar and Mishra, 2002). The curves shown in Figure 4(b) are temperature distributions obtained for $N = 0.001$ and two values of boundary emissivities: $\varepsilon = 1.0$ and $\varepsilon = 0.1$.

A uniform discretization with 100 strips is used. The number of iterations required for convergence varied between two and five, where the maximum value ($n = 5$) was necessary for the case with pure radiation ($N = 0$). A tolerance of 0.001 is used. As it can be seen in Figure 4(a), the results are in very good agreement with those published in Talukdar and Mishra (2002). Note the very low number of iterations required by the present model for the cases dominated by radiation. In Talukdar and Mishra (2002), for example, the number of iterations for $N = 0.1, 0.01, 0.001$ and 0.0001 was approximately 80, 120, 600 and 650, respectively, and under relaxation was necessary in that study for $N \leq 0.01$.

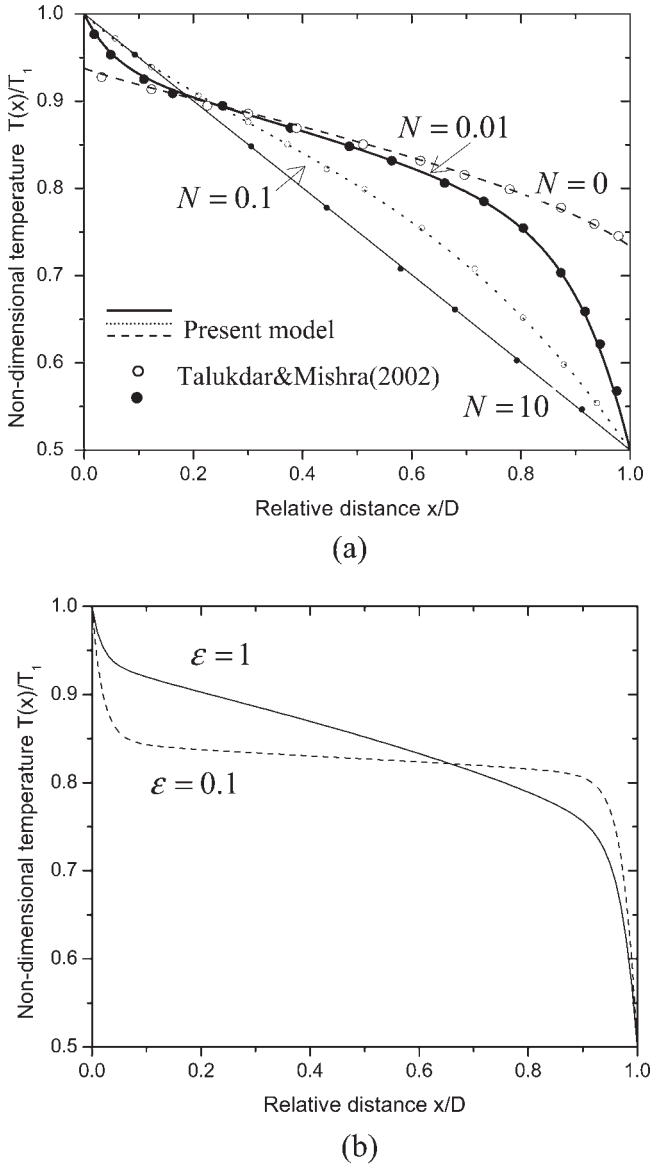


**Figure 4.**
Temperature distribution for the gray sample with $\kappa_D = 1$

**Notes:** (a) Boundary emissivities $\varepsilon = 1$; (b) boundary emissivities $\varepsilon = 1$ and $\varepsilon = 0.1$

Non-dimensional temperature fields in gray materials with different boundary emissivities and optical thicknesses, $T_1/T_2 = 0.5$, and $N = 0$ are shown in Figure 5. To verify the model in describing the heat transfer phenomena with only radiation, the temperature fields are compared with those resulting of (Viskanta and Grosh, 1962b). As it can be seen, the results are in good agreement and the largest difference corresponds to about 2.6 per cent for $\kappa_D = 10$. The maximum number of iteration was six and occurred

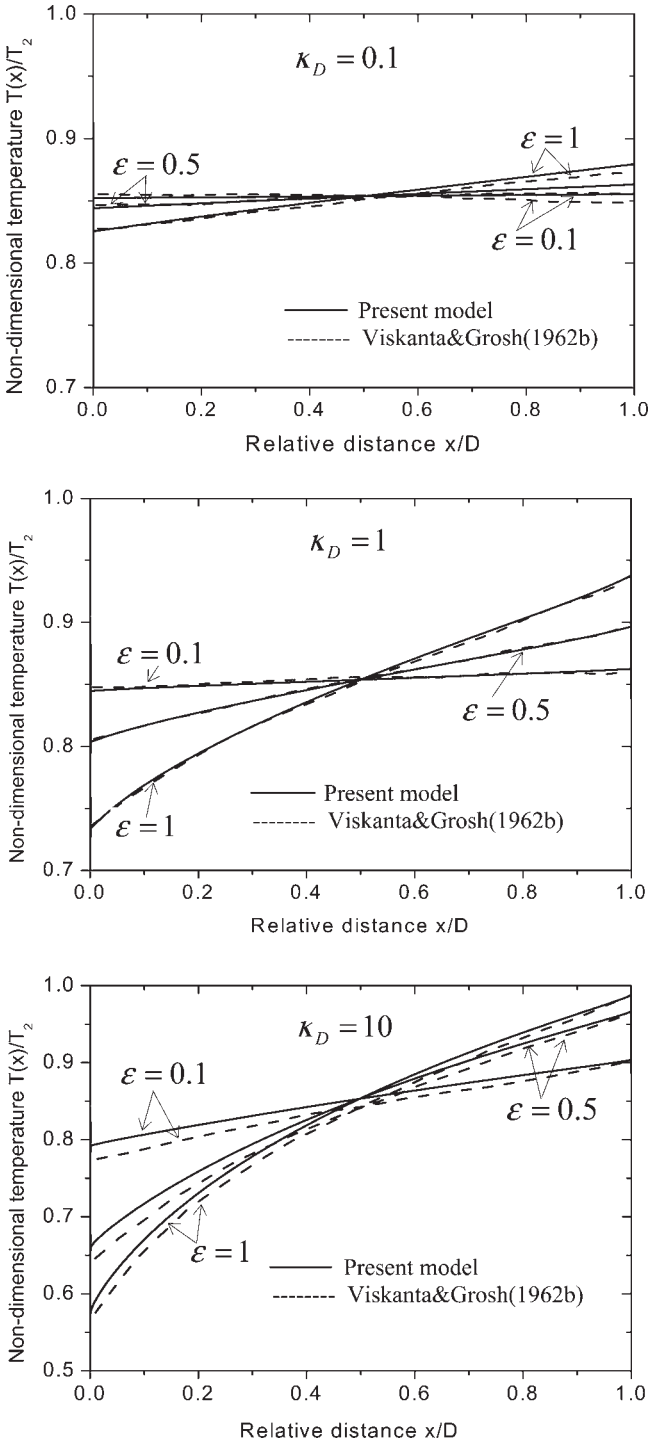


**Figure 5.**
Temperature along the gray sample for $N = 0$ and different optical thicknesses

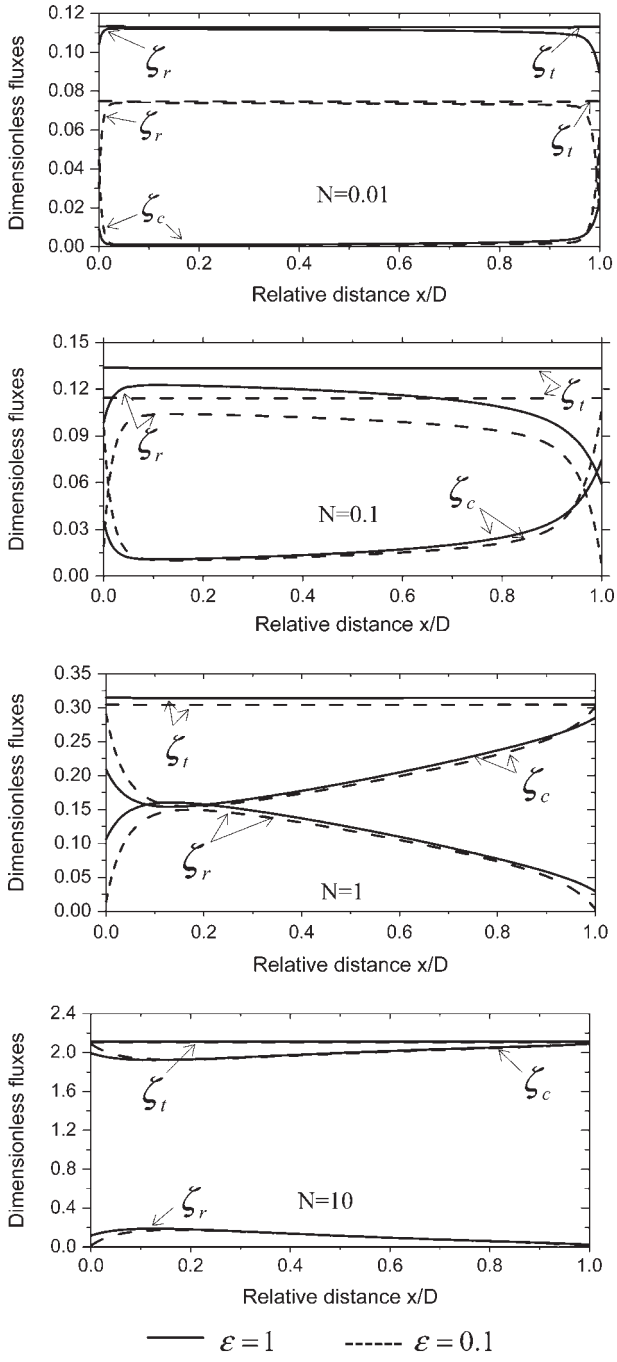


**Figure 6.**
Dimensionless heat fluxes along the gray samples

**Notes:** r = radiation, c = conduction, t = total

for the case $\kappa_D = 10$. For these cases, a more refined discretization was used to improve the heat flux results near the boundaries. Specifically, 50 strips uniformly distributed on each one of the two $0.01\kappa_D$ sized regions close to the boundaries and 200 strips on the rest of the sample width were used. For thick samples, a non-uniform discretization, refined toward the boundaries, is preferred in order to capture the radiation heat transfer that is stronger near the boundary. Oscillations of the calculated total flux can be used as an indicator of the need for refinement near the boundaries.

Non-dimensional heat fluxes obtained by the present model for gray material with optical thickness $\kappa_D = 10$, $T_2/T_1 = 0.5$ and different values of the conduction–radiation parameter are shown in Figure 6. Again, the emissivities of both the boundaries have been taken equal to $\varepsilon = 1.0$ and $\varepsilon = 0.1$, respectively. In Figure 6, the conductive, radiative and total non-dimensional fluxes are represented by $\zeta_c, \zeta_r$ and $\zeta_t$, respectively. A non-dimensional flux is defined by the relation $\zeta = q/(\sigma T_{ref}^4)$, where $q$ represents a real flux. A discretization with 200 strips is used, with 50 per cent of them uniformly distributed over the two regions of length 0.05D near the boundaries. The maximum number of iterations for convergence was five, for the case with only radiation ($N = 0$). For $N = 10$, the model need only two iterations for convergence. Again, a tolerance of 0.001 was used.

Numerical values of the non-dimensional total flux compared with those obtained by Viskanta and Grosh (1962b) are presented in Tables I and II.

## Application to non-gray materials

Silica aerogel is analyzed to demonstrate the model for non-gray material. Silica aerogels are materials that exhibit extinction coefficients strongly dependent on the electromagnetic wavelength (Heinemann *et al.*, 1996). A sample of silica aerogel

| $\kappa_D$ | $T_1/T_2$ | $N$ | Non-dimensional total heat flux | |
|---|---|---|---|---|
| | | | This study | Viskanta[a] |
| 0.1 | 0.5 | 0 | 0.858 | 0.859 |
| | | 0.01 | 1.079 | 1.074 |
| | | 0.1 | 2.876 | 2.88 |
| | | 1.0 | 20.846 | 20.88 |
| | | 10 | 200.540 | 200.88 |
| 1.0 | 0.1 | 0 | 0.559 | 0.556 |
| | | 0.01 | 0.631 | 0.658 |
| | | 0.1 | 0.968 | 0.991 |
| | | 1.0 | 4.192 | 4.218 |
| | | 10.0 | 36.546 | 36.6 |
| 1.0 | 0.5 | 0 | 0.519 | 0.518 |
| | | 0.01 | 0.567 | 0.596 |
| | | 0.1 | 0.769 | 0.798 |
| | | 1.0 | 2.570 | 2.60 |
| | | 10.0 | 20.54 | 20.60 |
| 10.0 | 0.5 | 0 | 0.109 | 0.102 |
| | | 0.01 | 0.113 | 0.114 |
| | | 0.1 | 0.133 | 0.131 |
| | | 1.0 | 0.315 | 0.315 |
| | | 10.0 | 2.111 | 2.114 |

**Source:** [a]Viskanta and Grosh (1962b)

**Table I.**
Values of non-dimensional total heat flux, $\varepsilon_1 = \varepsilon_2 = 1.0$

| $\kappa_D$ | $T_1/T_2$ | $N$ | Non-dimensional total heat flux This study | Viskanta[a] |
|---|---|---|---|---|
| 0.1 | 0.5 | 0 | 0.0491 | 0.049 |
| | | 0.01 | 0.277 | 0.267 |
| | | 0.1 | 2.074 | 2.078 |
| | | 1.0 | 20.044 | 20.08 |
| | | 10.0 | 200.00 | 200.08 |
| 1.0 | 0.1 | 0 | 0.061 | 0.051 |
| | | 0.01 | 0.198 | 0.22 |
| | | 0.1 | 0.570 | 0.591 |
| | | 1.0 | 3.809 | 3.752 |
| | | 10.0 | 36.15 | 36.22 |
| 1.0 | 0.5 | 0 | 0.0476 | 0.047 |
| | | 0.01 | 0.157 | 0.156 |
| | | 0.1 | 0.402 | 0.393 |
| | | 1.0 | 2.219 | 2.245 |
| | | 10.0 | 20.19 | 20.25 |
| 10.0 | 0.5 | 0 | 0.036 | 0.036 |
| | | 0.01 | 0.0874 | 0.090 |
| | | 0.1 | 0.114 | 0.115 |
| | | 1.0 | 0.304 | 0.297 |
| | | 10.0 | 2.102 | 2.107 |

**Table II.**
Values of non-dimensional total heat flux, $\varepsilon_1 = \varepsilon_2 = 0.1$

**Source:** [a]Viskanta and Grosh (1962b)

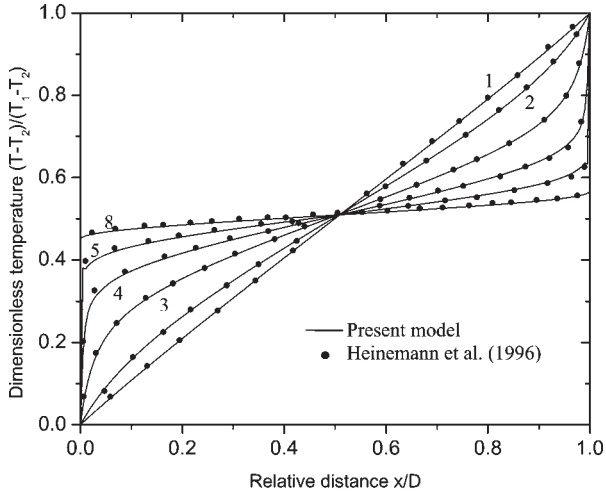


**Figure 7.**
Temperature variation along the aerogel sample for different values of the thermal conductivity

**Notes:** The curve labels indicate the exponent n in $\beta_c = 10^{-n}$ W/(m$^2$K)

0.0175 m thick with boundary temperatures $T_1 = 293$ K and $T_2 = 303$ K is analyzed. The specific extinction spectrum of the material can be found in (Heinemann *et al.*, 1996). The refractive index is equal to 1.00, independent of the wavelength, which is typical of silica aerogels. Six different values of thermal conductivities

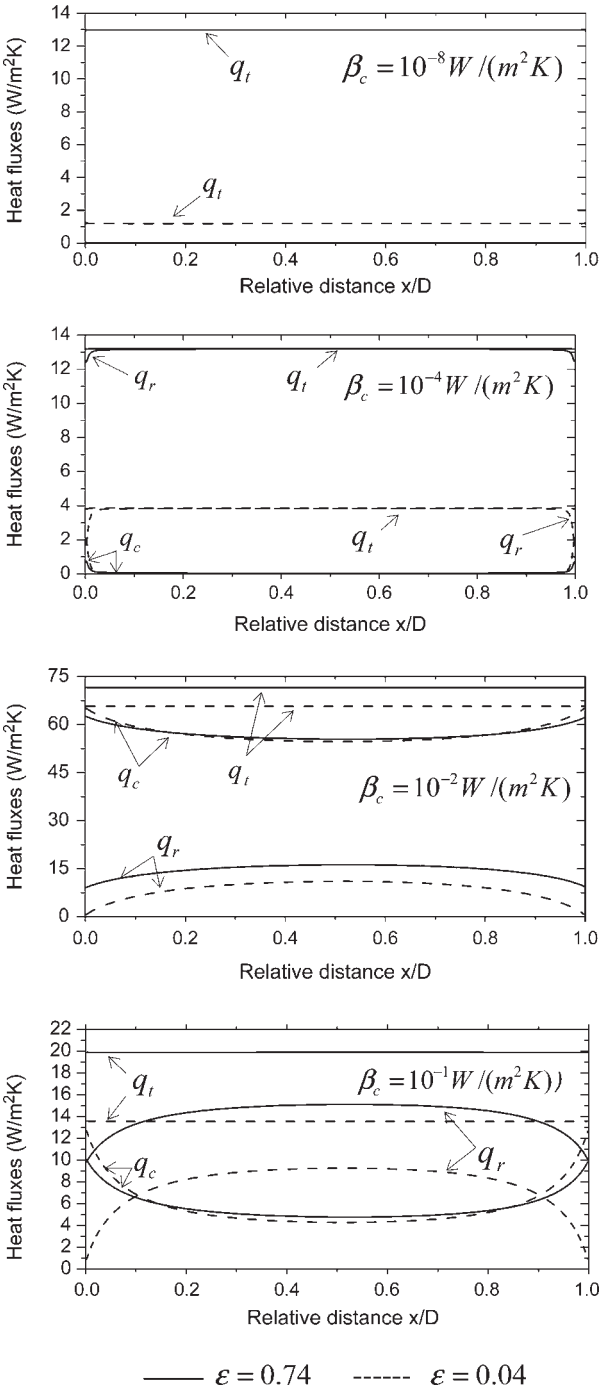


**Figure 8.**
Heat fluxes along the aerogel sample for different thermal conductivities

$\beta_c = 10^{-n}\ W/(m^2K)$ are considered, with $n = 1, 2, 3, 4, 5, 8$. The emissivity of the boundaries is 0.04. The sample was discretized into 200 strips, and the extinction spectrum was divided into 54 bands with variable widths in the interval $1.4\,\mu m \leq \lambda \leq 200\,\mu m$.

Temperature distribution through the thickness of the sample as a function of the relative position for the different thermal conductivity values are shown in Figure 7. The conductive, radiative and total heat fluxes, corresponding to thermal conductivities $\beta_c = 10^{-8}$, $10^{-4}$ and $10^{-1}$ W/(m$^2$K), are shown in Figure 8. The number of iterations required for convergence varied between two and five.

## Conclusion

A novel numerical formulation for the analysis of conduction–radiation heat transfer in one-dimensional planar absorbing, emitting, non-gray material is presented. The accuracy of the model is demonstrated by comparing results for gray and non-gray materials with prior results from the literature.

The computational efficiency of the formulation is verified for cases dominated by radiation and thick samples, which are very challenging to the heat transfer algorithms. The number of iterations required for convergence is low, even in cases dominated by radiation.

## References

Anteby, I., Shai, I. and Arbel, A. (2000), "Numerical calculations for combined conduction and radiation transient heat transfer in a semitransparent medium", *Numerical Heat Transfer, Part A*, Vol. 37, pp. 359-71.

Cavalcante, M.A.A., Marques, S.P.C. and Pindera, M.-J. (2007), "A parametric formulation of the finite-volume theory for functionally graded materials. Part 1: analysis", *Journal of Applied Mechanics – ASME*, Vol. 74, pp. 935-45.

Coelho, P.J. and Gonçalves, J. (1999), "Parallelization of the finite volume method for radiation heat transfer", *International Journal of Numerical Methods for Heat and Fluid Flow*, Vol. 9 No. 4, pp. 388-406.

Daurelle, J.-V., Occelli, R. and Jaeger, M. (1999), "Finite modeling of radiation in a nonparticipating medium coupled with conduction and convection heat transfer with moving boundaries", *International Journal of Numerical Methods for Heat and Fluid Flow*, Vol. 9 No. 3, pp. 257-70.

Heinemann, U., Caps, R. and Fricke, J. (1996), "Radiation–conduction interaction: an investigation on silica aerogels", *International Journal of Heat and Mass Transfer*, Vol. 39 No. 10, pp. 2115-30.

Manzari, M.T. (1998), "A mixed approach to finite element analysis of hyperbolic heat conduction problems", *International Journal of Numerical Methods for Heat and Fluid Flow*, Vol. 8 No. 1, pp. 83-96.

Marakis, J.G., Chamiço, J., Brenner, G. and Durst, F. (2001), "Parallel ray tracing for radiative heat transfer: application in a distributed computing environment", *International Journal of Numerical Methods for Heat and Fluid Flow*, Vol. 11 No. 7, pp. 663-81.

Mishra, S.C. and Prasad, M. (2002), "Radiative heat transfer in absorbing–emitting–scattering gray media inside 1-D gray Cartesian enclosure using the collapsed dimension method", *International Journal of Heat and Mass Transfer*, Vol. 45 No. 3, pp. 697-700.

Mishra, S.C., Roy, H.K. and Misra, N. (2006), "Discrete ordinate method with a new and a simple quadrature scheme", *Journal of Quantitative Spectroscopy and Radiative Transfer*, Vol. 101, pp. 249-62.

Mishra, S.C., Talukdar, P., Trimis, D. and Durst, F. (2004), "Effect of angular quadrature scheme on the computational efficiency of the discrete transfer method for solving radiative transport problem with participating medium", *Numerical Heat Transfer, Part B*, Vol. 46, pp. 463-78.

Ratzell III, A.C. and Howell, J.R. (1982), "Heat transfer by conduction and radiation in one-dimensional planar medium using differential approximation", *Journal of Heat Transfer – ASME*, Vol. 104, pp. 388-99.

Shah, N.G. (1979), "New method of computational of radiation heat transfer combustion chambers", PhD thesis, Imperial College, University of London, London.

Siegel, R. and Howell, J.R. (2002), *Thermal Radiation Heat Transfer*, 4nd ed., Taylor & Francis, New York, NY.

Talukdar, P. and Mishra, S.C. (2002), "Analysis of conduction-radiation problem in absorbing, emitting and anisotropically scattering media using the collapsed dimension method", *International Journal of Heat and Mass Transfer*, Vol. 45, pp. 2159-68.

Viskanta, R. and Grosh, R.J. (1962a), "Heat transfer by simultaneous conduction and radiation in an absorbing medium", *Journal of Heat Transfer–ASME*, Vol. 84, pp. 63-72.

Viskanta, R. and Grosh, R.J. (1962b), "Effect of surface emissivity on heat transfer by simultaneous conduction and radiation", *International Journal of Heat and Mass Transfer*, Vol. 5, pp. 729-34.

**Corresponding author**
Severino P. C. Marques can be contacted at: smarques@ctec.ufal.br